# Supporting Information

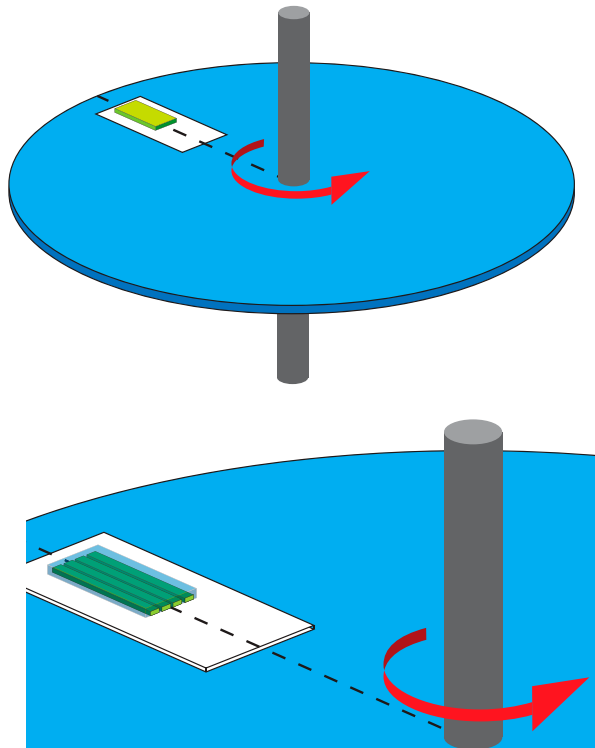## Saragosti et al. 10.1073/pnas.1101996108



**Fig. S1.** Centrifugation set-up. The array of microchannels is aligned with a radius of the spin-coater and positioned at *ca*. 9 cm from the rotation axis. Typical rotation velocity was 750 rpm (corresponding to 65 g).
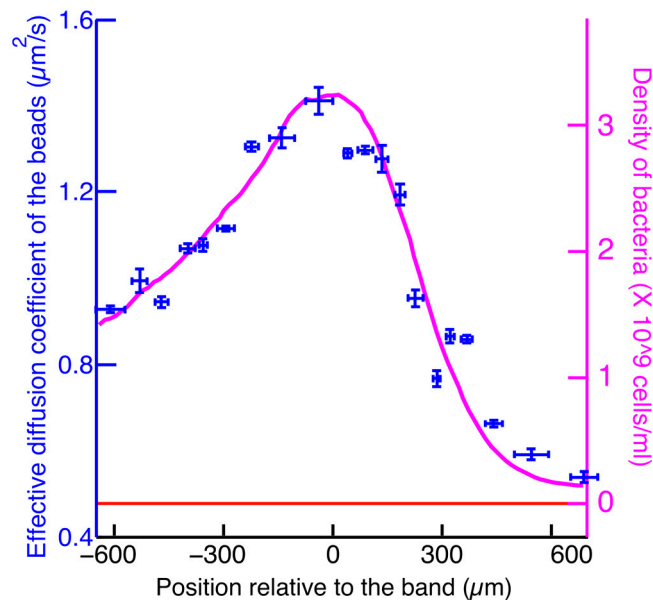


**Fig. S2.** Hydrodynamic contribution: Tracking of passive markers. Blue points: Coefficients of diffusion of 1 μm polystyrene micro beads as a function of their position in the bacterial wave. The concentration profile is superimposed (purple line). The values are obtained by fitting the mean square displacements calculated over the beads contained in each bin. The red line indicates the theoretical value of 0.44 μm²/s expected for 1 μm beads in the absence of bacteria. These diffusion coefficients are proportional to the local bacteria concentration. If the migrating population of bacteria did not induce a drift of the beads, it clearly enhanced diffusion. This effect would promote the dispersion of the traveling band and the bacterial waves have to overcome this additional agitation to last.

Motility buffer

Zone of observation

Motility buffer
+ 1mM D-Glucose

**Fig. S3.** Migration in an externally imposed gradient. The experimental set-up consisted in two wide chambers connected by a long and narrow channel (6 mm × 0.7 mm). Practically, we used 400 μm thick polydimethylsiloxane (PDMS) spacers manually cut to the right dimensions, between a glass slide and a cover slip. One of the chambers was filled with motility buffer with 1 mM D-Glucose and the other with a very dilute suspension of motile and fluorescent bacteria previously cultured at 30 °C in LB to an OD of 0.5, and then resuspended in motility buffer to an OD of 0.005. At these low concentrations, consumption of nutrients or oxygen is negligible. The trajectories were collected 30 min after inoculation, in the middle of the channel and analyzed following the exact same procedure as for the trajectories in the wave. The chemotactic bias was clear on the distribution of run durations (Fig. S4A). The angular distribution of the detected runs was also biased in the direction up the gradient (Fig. S4B) thus confirming the persistence mechanism evidenced in the present study.



**Fig. S4.** (A) Time distributions of the tumbles (black) and runs (green: positive direction, blue: perpendicular direction, red: negative direction) for very dilute suspensions of bacteria in an externally imposed D-Glucose gradient (Fig. S3). Runs are longer when up the gradient. $\tau_{tumble} = 0.12 \pm 0.01$ s; $\tau_{run} = 0.90 \pm 0.03$ s; $\langle\tau_{run}\rangle_+ = 1.12 \pm 0.03$ s; $\langle\tau_{run}\rangle_0 = 0.85 \pm 0.02$ s; $\langle\tau_{run}\rangle_- = 0.71 \pm 0.02$ s. The velocity remained unchanged ($V_{run}^{2D} = 18.4 \pm 7.9$ μm/s). (B) Angular distribution of the runs. Runs up the gradient are more probable than runs down the gradient.



**Fig. S5.** Traveling pulse with constant persistence ($\sigma = \sqrt{\langle\alpha^2\rangle} = 1.45$). A pulse travels at constant speed with a conserved profile. (A) Simulated kymograph = time/space representation of the bacterial density. (B) Snapshot of the bacterial density (pink) and the mean run times for bacteria moving to the left (red) and to the right (green) at time $t = 2,500$ s. The macroscopic velocity is 3.2 μm/s.

**Fig. S6.** Influence of the reorientation on the behavior of the cells in an imposed gradient. We assume an exponential gradient of nutrients along a channel of length $L$ ($L = 6$ mm) (e.g., glucose for a comparison with Fig. S3, although these particular experiments were conducted in a linear gradient): $N(x) = N_0 \cdot \exp(\alpha \cdot (x - L))$ with $\alpha = 2$ mm$^{-1}$ (this parameter has been chosen so that $\delta^{-1} \cdot v' \cdot \frac{d \operatorname{Log}(N)}{dx} \sim 1$). $\alpha$ is analog to the "constant-activity gradient" defined in ref. 1 below. In these simulations, the tumble frequency is 1.15 s$^{-1}$ (experimentally measured in the conditions of Fig. S3), $\chi_S = 0$ (the bacteria are too diluted to interact by the secreted chemoattractants) and we neglect division ($r = 0$). All the other parameters are the same as in Table 1. The bacteria in the glucose-free reservoir are modeled by a constant source. In these conditions, we observe a propagating front (from left to right). We have compared three different situations differing by the modulation of the reorientation. $\sigma_1$ is the extreme value determined from the experiments described in Fig. S3. $\sigma_2 = 0$ (absence of modulation of the reorientation) leads to a small velocity for the progression of the bacteria: $v \sim 2.6 \mu$m/s. This velocity increases with $\sigma_2$: $\sigma_2 = 0.4$ corresponds to the value experimentally measured in the experiments in the linear gradient, this value yields a velocity of ca. 4 $\mu$m/s, larger than in the absence of modulation but smaller than the experimental value of 5.5 $\mu$m/s. This observation is not surprising as the shapes of the two gradients are very different. The experimental value is recovered by arbitrarily setting $\sigma_2$ to 0.85. Interestingly, this same value is also the one that fits best the asymmetric angular distribution of the runs. We note that the run durations to the left or to the right are unaffected by the modulation ($\langle \tau_{\text{run}} \rangle_+ \sim 1.1$ s; $\langle \tau_{\text{run}} \rangle_- \sim 0.7$ s).

1  Vladimirov N, et al. (2010) Predicted auxiliary navigation mechanism of peritrichously flagellated chemotactic bacteria. *PLoS Comp Biol* 6:e1000717.